10 Superconductivity and Magnetism

D.G. Eshchenko, H. Keller, R. Khasanov (till December 2007), F. La Mattina, A. Maisuradze, J. Roos, S. Strässle, St. Weyeneth, B.M. Wojek, C. Duttwyler (Master student), U.. Mosele (Master student), M.V. Eremin (visiting scientist), V.B. Graneli (visiting scientist), A. Ivanshin (visiting scientist), B. Kochelaev (visiting scientist), R. Pusniak (visiting scientist), A. Shengelaya (visiting scientist)

Emeritus members:
Prof. K.A. Müller (Honorarprofessor), Prof. T. Schneider (Titularprofessor), Dr. M. Mali

in collaboration with: ETH Zürich (K. Conder, J. Karpinski), Paul Scherrer Institute (K. Conder, E. Morenzoni), Max-Planck-Institute for Solid State Research Stuttgart (A. Bussmann-Holder), IBM Rüschlikon Research Laboratory (J.G. Bednorz, S.F. Alvarado), University of Geneva (Ø. Fischer, J.M. Triscone), University of Rome (D. Di Castro), Kazan State University (A. Dooglav, M.V. Eremin, V. Ivanshin, B.I. Kochelaev), Polish Academy of Sciences (R. Puzniak), University of Belgrade (I.M. Savić), Tbilisi State University (A. Shengelaya), Russian Research Centre "Kurchatov Institute" (V.G. Storchak), Osaka University (S. Tajima), University of Tokyo (T. Sasagawa, H. Takagi), University of British Columbia (J.H. Brewer), Iowa State University (A. Kaminski).

We continued our research on magnetic and electronic properties of novel materials during the last year. In our efforts we profit from synergy effects in combining complementary experimental techniques, including muon-spin rotation (μSR), electron paramagnetic resonance (EPR), nuclear magnetic resonance (NMR), nuclear quadrupole resonance (NQR), as well as SQUID and torque magnetometry. Most prominent examples of our studies are presented in the following sections.

10.1 Two-gap superconductivity in cuprate superconductors

In collaboration with other research groups we recently performed two decisive experiments on cuprate high temperature superconductors (HTS's) which challenge theoretical models based on purely electronic mechanisms. From muon spin rotation (μSR) experiments the temperature dependence of the superfluid density has been determined from which clear conclusions on the pairing symmetry can be extracted. The experimental results for three different cuprate families disclose generic trends for HTS's, namely the coexistence of an s-wave and a d-wave gap in the CuO_2 planes and a predominantly s-wave gap along the c-axis (1; 2; 3) (Figs. 10.1 and 10.2 show representative results). These findings are not compatible with approaches that concentrate on the planes only, but consistent with early predictions where the 3D nature of high temperature superconductivity was suggested to be manifest in coupled gaps (4; 5). In addition, the existence of the s-wave gap is in strong support of ideas that the lattice plays a crucial role in HTS's. These latter conclusions are in accord with oxygen isotope effect (OIE) experiments where not only OIE's on the superconducting transition temperature but also on the magnetic penetration depth (6), the superconducting gaps, the Néel temperature, and the spin glass temperature have been observed (7). Throughout the whole phase diagram of cuprates OIE's exist which are sign reversed for the superconducting properties as compared to the magnetic states. The strong doping dependence of these OIE's has been shown to stem from renormalizations of the kinetic energy

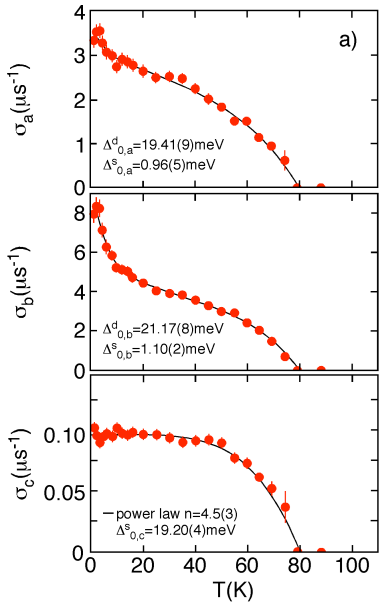

Figure 10.1: Temperature dependence of the μSR relaxation rates $\sigma_a \propto \rho_a$, $\sigma_b \propto \rho_b$, and $\sigma_c \propto \rho_c$ of single crystals of $YBa_2Cu_4O_8$ measured along the crystallographic directions a, b, and c (ρ_a, ρ_b, and ρ_c are the corresponding superfluid densities) [3]. Individual values of the s- and d-wave gap are indicated. The full lines are results from a power law dependence [2].

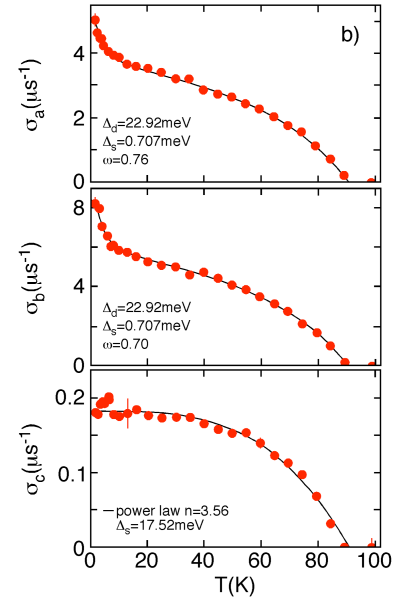

Figure 10.2: The same as in Fig. 10.1 but for $YBa_2Cu_3O_{7-\delta}$ [2].

caused by polaron formation (8). This interpretation is consistent with ideas that led to the discovery of high temperature superconductivity, namely the concept of Jahn-Teller polarons (9) which might provide a much better glue to the electron pairing than conventional electron-phonon coupling. Since both above mentioned experiments are direct, bulk sensitive, and unambiguous and have been carried through systematically for different cuprate families and as functions of doping, we conclude that the order parameter in cuprates is much more complex than just d-wave symmetry, the third dimension, i.e., physics involving the c-axis are of outermost importance, lattice effects in terms of polaron formation crucially dominate the whole phase diagram.

[1] R. Khasanov, A. Shengelaya, A. Maisuradze, F. La Mattina, A. Bussmann-Holder, H. Keller, and K. A. Müller, Phys. Rev. Lett. **98**, 057007 (2007).

[2] R. Khasanov, S. Strässle, D. Di Castro, T. Masui, S. Miyasaka, S. Tajima, A. Bussmann-Holder, and H. Keller, Phys. Rev. Lett. **99**, 237601 (2007).

[3] R. Khasanov, A. Shengelaya, A. Bussmann-Holder, J. Karpinski, H. Keller, and K. A. Müller, J. Supercond. Nov. Magn. **21**, 81 (2008).

[4] K.A. Müller, Nature (London) **377**, 133 (1995).

[5] K.A. Müller and H. Keller, in **High T_c Superconductivity 1996: Ten Years after the Discovery** (Kluwer, Dordrecht, 1997) p. 7.

[6] See e.g., H. Keller, in **Superconductivity in Complex Systems**, eds. K.A. Müller and A. Bussmann-Holder (Springer Series Structure and Bonding) **114**, 143 (2005); and refs. therein.

[7] R. Khasanov, A. Shengelaya, D. Di Castro, E. Morenzoni, A. Maisuradze, I.M. Savic, K. Conder, E. Pomjakushina, H. Keller, arXiv:0711.2257.

[8] A. Bussmann-Holder and H. Keller, in **Polarons in Advanced Materials**, eds. A.S. Alexandrov (Springer Series in Materials Science 103, Canopus Publishing, Bristol 2007), pp. 599.

[9] K.A. Müller, J. Phys. C: Condens. Matter **19**, 251002 (2007) and refs. therein.

10.2 Superconductivity and magnetism in $YBa_2Cu_3O_7/PrBa_2Cu_3O_7$ multi-layers

Heterostructures consisting of magnetic and superconducting layers juxtaposed to each other are ideal systems to investigate the interplay (coexistence, competition) of the two order parameters and to study possible interlayer coupling. These properties have been subject of intense research in the recent years. For instance in superlattices composed of one unit cell thick layers $YBa_2Cu_3O_7$ (YBCO) separated by $PrBa_2Cu_3O_7$ (PBCO) layers of variable thickness the critical temperature of the heterostructure has been found to decrease continuously as the PBCO thickness is increased indicating that coupling persists over distances of approximately 10 nm (1).

We used spin polarized low energy muons to investigate the local superconducting and magnetic properties of c-axis oriented $YBa_2Cu_3O_{7-\delta}$/ $PrBa_2Cu_3O_{7-\delta'}$/ $YBa_2Cu_3O_{7-\delta}$ tri-layers as well as of a $YBa_2Cu_3O_{7-\delta}$/ $PrBa_2Cu_3O_{7-\delta'}$ bi-layer system and single layer films of the constituents. Low energy μSR offers the unique possibility to measure local fields on a nanometer scale (2), to determine the spatial distribution of the magnetization throughout the layers, and to identify superconducting and magnetic fractions, quantities about which very little is known in multilayers.

In a series of measurements we investigated the response of the heterostructures to an external perturbation represented by a magnetic field applied parallel to the surface (and parallel to the ab-planes). In the trilayer we find that below the critical temperature of YBCO, a sizeable fraction of the PBCO buffer layer displays a diamagnetic shift characteristic of the superconducting state. This fraction is coexisting with an antiferromagnetic fraction.

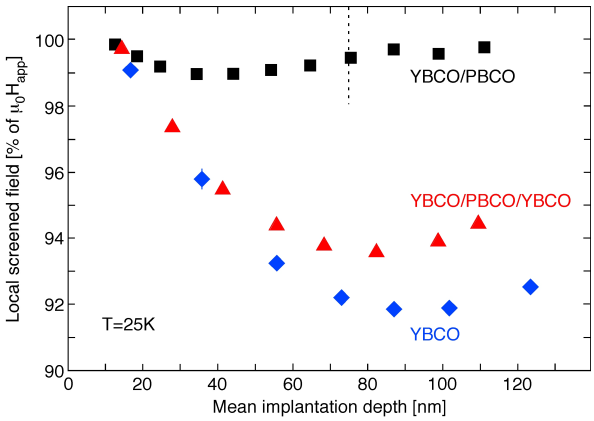

Figure 10.3: Depth dependence of the local screened magnetic field in the bi-layer (black squares) and tri-layer (red triangles) samples at T=25 K in the Meissner state. The dotted line indicates the top YBCO/PBCO interface. For comparison the depth profile of a 200 nm thick single layer of YBCO is also shown (blue diamonds).

A typical depth profile of the diamagnetically shifted field component is depicted in Fig. 10.3 at a temperature below the critical temperature of YBCO. In the YBCO/PBCO/YBCO film the monotonic decrease of the screened field in the top superconducting layer and the large shift in PBCO imply that unexpected large supercurrents with no dissipation are flowing through a 50 nm AF barrier to the bottom YBCO layer, which sustains the return flow. The absence of a second superconducting layer suppresses the back flow and hence the observed diamagnetic shift in PBCO, possibly indicating that the induced superfluid density in PBCO is much lower than in YBCO and that the effective penetration depth in PBCO is much larger than in the superconductor, where from our measurement we determine $\lambda_{ab} \simeq 200$ nm.

By applying a magnetic field perpendicular to the surface and to the ab-planes we observed the typical field distribution of a rigid vortex state in the top and bottom superconducting layer, reflecting the vortex supercurrents flowing in the ab-planes. From a detailed analysis of the field distribution observed at

various depths, we expect to quantify the amount of superfluid density induced in the barrier layer. Although the mechanism of our observation is not understood in detail at the moment, the results present the signature of a large proximity effect between two compounds with different electronic ground state, not expected on the base of conventional proximity theory. The results call for additional investigations. We plan to measure the effect as a function of the thickness of the single components and extend the investigations to other cuprates (e.g. of the 214 family) where we have recently observed similar effects with strongly underdoped barriers and where so-called giant proximity effects in the Josephson current have been reported (3).

[1] J.-M. Triscone and Ø. Fischer, Rep. Prog. Phys. **60**, 1673 (1997).

[2] E. Morenzoni, R. Khasanov, T. Luetkens, H. Prokscha, and A. Suter, J. Neutron Research **14**, 269 (2006).

[3] I. Bozovic, G. Logvenov, M. A. J. Verhoeven, P. Caputo, E. Goldobin, and M. R. Beasley, Phys. Rev. Lett. **93**, 157002 (2004).

10.3 Spectroscopic studies of novel electronic materials

10.3.1 Antiferromagnetic to superconducting phase transition in $Y_{0.98}Yb_{0.02}Ba_2Cu_3O_x$ for $x \simeq 6.4$ investigated by Yb^{3+} EPR

The antiferromagnetic (AF) to superconducting (SC) phase transition in $YBa_2Cu_3O_x$ for $x \simeq 6.4$ is subject of recent studies (1; 2; 3). Whereas superconductivity in $La_{2-x}Sr_xCuO_4$ emerges from a nonmetallic phase, the precursor phase for $YBa_2Cu_3O_x$ remains still controversial. A detailed study in the vicinity of the boundary between AF and SC phases is needed to understand whether the AF and SC phases coexist, compete, or are separated by a novel phase. We report on the detailed investigation of $YBa_2Cu_3O_{6.4}$ by the Yb^{3+} EPR probe across the transition from the AF to the SC state. The AF to SC phase transition was induced by varying the hole concentration p in the CuO_2 planes near the critical concentration $p = 0.05$ holes/Cu where superconductivity appears/vanishes. To change the value of p the well known effect of its dependence on the chain-oxygen order was used. It was found that the width of the distribution of the oxygen content x of any investigated powder sample is less than 0.02 (80% of the sample's powder grains have an oxygen content in this range). Within the doping range $x \simeq 6.37 - 6.47$ the Yb^{3+} EPR line is split into a broad and a narrow component, unambiguously indicating the presence of an electronic phase separation. By comparing this result with neutron investigations of Ref. (2) we could assign the broad and the narrow EPR line to the central mode and the damped mode of the Cu spin dynamics of the neutron spectra, respectively.

By studying the temperature dependence of the linewidth of the broad Yb^{3+} signal it was possible to estimate the energy of the central mode to $E \simeq 0.03$ meV above 20 K. Below 20 K this energy gradually drops to zero. Our present result is in full agreement with studies of Sanna **et al.** suggesting a stripe-like order of carriers for $x \simeq 6.37 - 6.47$ (1).

[1] S. Sanna, G. Allodi, G. Concas, A.D. Hillier, and R. De Renzi, Phys. Rev. Lett. **93**, 207001 (2004).

[2] C. Stock, W.J.L. Buyers, Z. Yamani, C.L. Broholm, J.-H. Chung, Z. Tun, R. Liang, D. Bonn, W.N. Hardy, and R.J. Birgeneau, Phys. Rev. B **73**, 100504 (2006).

[3] M. Sutherland, S.Y. Li, D.G. Hawthorn, R.W. Hill, F. Ronning, M.A. Tanatar, J. Paglione, H. Zhang, L. Taillefer, J. DeBenedictis, R. Liang, D.A. Bonn, and W.N. Hardy, Phys. Rev. Lett. **94**, 147004 (2005).

10.3.2 Charge effects in $LaBa_2Cu_3O_{7-\delta}$

The study of charge effects in cuprates by means of ^{139}La NMR/NQR on $LaBa_2Cu_3O_{7-\delta}$ powder samples was completed with measurements of the temperature dependence of the three ^{139}La NQR resonance lines in the normal conducting phase. We observed a smooth increase of line frequencies with decreasing temperature that can be simply attributed to the shrinking of the lattice. Moreover, the complex temperature behavior of the ^{139}La nuclear spin-spin relaxation (NSSR) rate in the normal conducting phase was reinvestigated in more detail. We performed new NQR-NSSR measurements on lose powder samples which had been exposed to dry air for some month, however belonging to the same batch as the aligned powder samples which were used in our earlier NMR-NSSR investigation on c-axis aligned powder samples (cast in epoxy) (1). The pronounced steps and plateaus in the temperature dependent NMR-NSSR rate observed previously (1) are not present in the new NQR-NSSR data. From these findings we conclude that the previously observed complex NSSR temperature dependence is dominated by the long term behavior of the dynamics related to oxygen diffusion and reordering in the CuO-chains of $LaBa_2Cu_3O_{7-\delta}$.

In addition we extended the temperature range of our measurements of ^{139}La NMR parameters on c-axis aligned powder samples down to 2 K. Most interestingly we found that the nuclear spin-lattice relaxation rate for a magnetic field orientation parallel to the c-axis follows the same nearly linear temperature dependence ($\propto T^{4/3}$) which we observed in our earlier investigations at higher temperatures in the superconducting phase.

[1] S. Strässle , J. Roos , M. Mali , K. Conder, E. Pomjakushina, and H. Keller,
Physica C **460-462**, 890 (2007).

10.4 3D-xy critical properties in the fluctuation regime of the superconductor MgB_2

The observation of thermal fluctuation effects have been limited in conventional low-T_c superconductors because the large correlation volume makes these effects very small compared to the mean-field behavior. By contrast, the high transition temperature T_c and small correlation volume in a variety of cuprate superconductors lead to significant fluctuation effects (1; 2). In MgB_2 the correlation volume and T_c lie between these extremes, suggesting that fluctuation effects will be observable if measurements are done carefully enough.

We analyzed reversible magnetization data of a high quality MgB_2 single crystal in the vicinity of the zero field transition temperature, $T_c \simeq 38.83$ K. Though MgB_2 is a two gap superconductor our scaling analysis uncovers below T_c remarkable consistency with 3D-xy critical behavior similar to the situation in the cuprate superconductors. For this reason the magnetic field induced finite size effect, whereupon the correlation length transverse to the applied magnetic field cannot grow beyond a limiting magnetic length L_H, can be verified and studied in detail. Indeed, as the magnetic field increases, the density of vortex lines becomes greater, but not indefinitely. The limit is roughly set by the proximity of vortex lines due to the overlapping of their cores. This finite size effect implies that in type II superconductors, superconductivity in a magnetic field is confined to cylinders with diameter L_H. Accordingly, there is below T_c a 3D to 1D crossover line. It circumvents the occurrence of the continuous phase transition in the (H,T) -diagram along the H_{c2}-lines predicted by the mean-field treatment (3).

[1] T. Schneider and J.M. Singer, Phase Transition Approach To High Temperature Superconductivity, (Imperial College Press, London, 2000).

[2] T. Schneider, in: The Physics of Superconductors, edited by K. Bennemann and J.B. Ketterson (Springer, Berlin), p. 111 (2004).

[3] S. Weyeneth, T. Schneider, N.D. Zhigadlo, J. Karpinski, and H. Keller, J. Phys.: Condens. Matter **20**, 135208 (2008).

10.5 Charge transfer processes during resistive switching in Cr-doped $SrTiO_3$

Current induced bistable resistance effects in metal-insulator-metal structures involving transition-metal oxides and more recently also perovskite oxides such as $SrTiO_3$ have attracted substantial interest because of their potential technological applications for non-volatile memory devices. We investigate single crystals of Cr-doped $SrTiO_3$ as a model system for perovskite oxides exhibiting resistive memory behavior in the current-voltage characteristic (I-V). We found evidence of charge transfer processes involving the Cr site during the resistive memory switching of Cr-doped $SrTiO_3$. Electroluminescence (EL) was observed in-situ during I-V measurements. Our luminescence measurements performed on $SrTiO_3$:Cr crystals at different stages of conductivity reveal that the light emission is associated with 3d intrashell transitions of Cr^{3+} on an octahedral lattice site. Electrically stimulated emission can be taken as proof of dynamic processes involving trapping and subsequent radiative decay of electrons at the Cr dopant sites. With increasing conductivity of $SrTiO_3$ the emission maximum changes from the predominant well known R-line to another intrashell transition of Cr^{3+}(5). We interpret this as being due to a geometrical change of the oxygen octahedron, through either distortion and/or a modified oxygen vacancy distribution. The EL in the final state, which occurs only when the memory cell is switched from the low- to the high-resistance state, can provide an important stimulus for the refinement of theoretical models by taking controlled and defined trapping centers into account. Even if some models of the resistive switching on $SrTiO_3$ are presently under discussion, a conclusion about the role and the nature of intrinsic defects or dopants has not been done. Extended defects like dislocations and local changes of the oxygen vacancy content has been proposed to be responsible for the conduction in $SrTiO_3$ (1; 2). Inhomogeneity of the crystal in the bistable conductive state has been shown experimentally (3) as a property arising from the forming procedure, and a phenomenological model (4) points out the requirement of extended non percolating domain structures. However a clear explanation of the role of the Cr dopant has not been incorporated in any models. We found an essential process describing the decreases of conductivity during the resistive switching, which involves the Cr site as a reversible trapping center for the conducting electrons (5).

[1] M. Janoush, G.I. Meijer, U. Staub, B. Delley, S.F. Karg, and B.P. Andreasson, Adv. Mater. **19**, 2232 (2007).

[2] K. Szot, W. Speier, G. Bihlmayer, and R. Waser, Nature Mater. **5**, 312 (2006).

[3] C. Rossel, G.I. Meijer, D. Brémaud, and D. Widmer, J. Appl. Phys. **90**, 2892 (2001).

[4] M.J. Rozenberg, I.H. Inoue, and M.J. Sánchez, Phys. Rev. Lett. **92**, 178302 (2004).

[5] S. F. Alvarado, F. La Mattina, and J.G. Bednorz, Appl. Phys. A **89**, 85 (2007).